Diffusion chronometry and the timescales of magmatic processes

F. Costa[1,2]✉, *T. Shea*[3] *and T. Ubide*[4]

Abstract | Volcanic eruptions can represent major societal hazards. Placing tighter bounds on the timescales of magmatic processes that precede eruptions is, therefore, important for volcano monitoring and forecasting. Diffusion chronometry, where volcanic crystals that contain chemical gradients are treated as time capsules, allows the timescale of various magmatic processes to be constrained. In this Review, we discuss the basics of diffusion chronometry and describe how re-equilibration via chemical diffusion provides insights into the timescales of magma storage, ascent and eruption. Crystals from mafic volcanoes record timescales of days to years between magma intrusion and eruption, which broadly match those recorded by monitoring data (such as increased seismicity). The timescales recorded in crystals from large silicic calderas, however, are typically longer than those from mafic volcanoes, spanning decades to millennia, but almost two orders of magnitude shorter than the timescales obtained by U-Th isotope disequilibria in zircon. The cause of this discrepancy is debated but likely reflects the protracted magma accumulation and complex thermal history that many crystals experience before eruption. Diffusion chronometry adds the fourth dimension to volcano science (that is, time), and advances in analytical and experimental approaches (such as NanoSIMS) open up new opportunities for understanding magmatic systems.

Diffusion coefficient
The constant of proportionality between the mass flux of elements through a given surface and the gradient of concentration due to elemental diffusion.

[1]*Earth Observatory of Singapore, Nanyang Technological University, Singapore, Singapore.*

[2]*Asian School of the Environment, Nanyang Technological University, Singapore, Singapore.*

[3]*Department of Earth Sciences, University of Hawai'i at Manoa, Honolulu, HI, USA.*

[4]*School of Earth and Environmental Sciences, The University of Queensland, St Lucia, Queensland, Australia.*

✉*e-mail: fcosta@ntu.edu.sg*

https://doi.org/10.1038/s43017-020-0038-x

Magmatic processes have traditionally been studied through the 'chemical-equilibria paradigm'[1,2], where phase-equilibria experiments[3], and thermodynamic modelling of multicomponent melts and minerals[4], represent the primary methods by which magma pre-eruptive storage conditions and processes are constrained. Combining experiments and/or thermodynamic models with petrological and chemical analysis of erupted minerals and melt inclusions forms the basis for unravelling the structure of the magmatic plumbing system below a given volcano[5,6] (FIG. 1). However, the textural and petrological record preserved in volcanic crystals and rocks demonstrates that equilibrium in natural systems is rarely achieved, and, therefore, other experimental and modelling approaches are required to fully understand sub-volcanic systems[3,7–12].

The presence of disequilibria in magmatic systems opens the way to the field of kinetics, through which the rate that a system departs from and attains new equilibrium can be studied. The relaxation of chemical gradients in crystals and glass through the diffusion of molecules or elements permits time information to be extracted from a range of magmatic processes through a technique termed diffusion chronometry[13–17]. Early applications of diffusion chronometry include the extraction of cooling-rate information from meteorites and lava lakes[18–20], as well as the development of an analytical solution to the diffusion equation to constrain the cooling histories of metamorphic rocks[21].

Owing to the increasingly precise experimental and improved theoretical constraints on the diffusion coefficient of key elements in volcanic minerals (such as Fe-Mg in olivine) and melts, the application of diffusion chronometry to magmatic and volcanic processes is now possible[22]. Concurrently, continued development of multiple analytical techniques has enabled precise and high-resolution analysis (typically between 100 µm and <1 µm) of the elemental and isotopic composition of volcanic minerals and glass to become routine[23–25]. Temporal and rate information derived from diffusion chronometry (and other methods of constraining magmatic time) enable quantification of storage and transport timescales in the crust, offer new insights into the relationship between magmatic processes and geophysical unrest signals, and provide critical time information for hazard mitigation at dormant volcanoes (FIG. 1).

In this Review, we discuss the techniques that are commonly used to constrain the timescales of magmatic processes, particularly U-Th-Ra dating of young zircons and some silicates[26–28], and summarize the basics of diffusion chronometry. In addition, we highlight the applications of diffusion chronometry in both mafic and

Key points

- Diffusion modelling of the chemical gradients in crystals can be used to extract invaluable time information from magmatic systems.
- Crystals from mafic volcanoes record the timescales of magma and transfer towards eruption that correlate with surface-monitoring data.
- Crystals from silicic volcanoes record timescales of magma remobilization and storage on the order of decades to hundreds of years, much shorter than U-Th dating of zircons.
- Further studies that integrate diffusion chronometry, using a wide range of elements and minerals, with thermal models of magmatic systems are required to understand the timescales of magma storage and remobilization.

silicic systems. The applications reviewed here demonstrate that diffusion chronometry — in combination with radiogenic dating via the U-Th-Ra disequilibria series — provides a detailed, though currently debated, image of magma residence in the crust prior to eruption. We finish by summarizing the main challenges and opportunities that are associated with the continued development of diffusion chronometry.

Approaches to obtain timescales

Various techniques have been developed to enable the timescales of magmatic processes to be recovered. Experimental calibrations of the kinetics of crystallization and bubble nucleation, as well as the U-Th-Ra disequilibrium-series method, have been successfully applied to magmatic systems for more than 30 years[29–31]. Below, we summarize these approaches and note some of their advantages and disadvantages.

Mineral and bubble textures

As magma decompresses towards the surface, water loss drives nucleation and growth of crystals and bubbles in the melt. Textural analysis of bubbles and/or crystals formed by decompression can be used to determine magma-ascent rates prior to eruption[5]. For example, microlites, which are small (typically <100 μm) crystals in the groundmass of volcanic products, can form by both cooling and decompression-induced degassing of magma[32]. Microlite textures (that is, their size, number, shape and distribution) have been used to extract information on the timescale of ascent and/or of the cooling of magmas from storage to the surface. Most texture-based techniques require experimental calibrations of crystal nucleation and growth rates, which have been done on a variety of melt compositions over the last four decades (reviewed in REF.[33]). Experimental data confirm that microlite nucleation and growth rates are dependent on the cooling and/or decompression rate of magma[32]. However, magma-decompression experiments also reveal that microlite-growth rates may vary by several orders of magnitude during magma storage and ascent[33]. Hence, crystal-growth rates need to be considered with caution when used to estimate timescales of magma ascent and/or cooling. Nevertheless, under conditions of no decompression and low undercooling at depth, crystal-growth rates vary within only one order of magnitude[34] and the total growth duration can be calculated more robustly.

Magma-decompression rates can also be calculated on the basis of vesicle textures in erupted pyroclasts, which can be converted into ascent rates if the crustal pressure gradient is known or some reasonable assumption can be made[35]. Bubble nucleation occurs owing to the decrease in volatile solubility associated with magma decompression. Nucleation rates are largely controlled by the magnitude and duration of decompression, as well as the rate at which volatiles can diffuse to a bubble nucleus[36]. Building on the classical nucleation theory, relationships between the number of bubbles and decompression rates have been calibrated for various magma compositions[37]. Therefore, the number of vesicles per unit volume melt in erupted pyroclasts can be used to calculate magma-decompression rates. However, it is necessary to assume that bubbles nucleate either homogeneously (without mineral substrates) or heterogeneously (aided by a mineral substrate), and the assumption made will greatly alter the values retrieved by this method[38]. As a result, there are still important limitations to the use of vesicle textures as a measure of magma-ascent rates.

Insights into the timescales of magmatic processes can also be derived by measuring the thickness of crystal-growth rims. Rim-thickness measurements offer a powerful method for constraining the approximate timescales of magma mobilization prior to eruption, provided that continuous crystal growth during low undercooling can be identified based on crystal shape and composition[39,40]. Similarly, the stability of hydrous minerals, such as amphibole, are sensitive to the amount of water in the melt and, therefore, to ambient pressure. In deep-seated magma-storage regions, water-rich magmas stabilize hydrous minerals[41]. However, as magmas ascend towards the surface, pressure decreases, water exsolves from the melt and hydrous minerals become unstable. Breakdown of amphibole, induced by decompression and H_2O loss, results in the formation of reaction rims formed from pyroxene, plagioclase, Fe-Ti oxides and melt. Experimental calibrations can then be used to convert reaction-rim thicknesses into the time available for magma ascent[42]. For example, reaction-rim measurements have been used to calculate decompression rates of 0.001–1 MPa s^{-1} for the 1980 eruption of Mount St Helens[42], the 1989 eruption of Mount Redoubt[43] and the 1997 eruption at Soufriere Hills volcano[44], which display a wide range of eruption styles. However, once the thickness of the rim becomes large enough to preclude further reaction with the surrounding melt, the assumption that the thickness of the mineral reaction rim is linearly proportional to time could result in the total ascent time being underestimated.

U-series short-lived isotopes

Chronometers based on textural analysis of bubbles and/or mineral phases can be used to constrain the relative timescales of magmatic processes, independent of the age of the rock and/or process that they track. By contrast, the decay of radiogenic isotopes provides a mechanism to track the absolute age of magmatic processes (such as a crystallization age). Radiometric dating of minerals and rocks has been widely used to infer rates of several geological processes[30,45]. However, analysis of radiogenic isotopes from the U-Th-Ra disequilibria series

Classical nucleation theory
Thermodynamic formalism where the free energy of formation of a mineral or bubble nucleus of critical size overcomes the energy associated with creating a new interface.

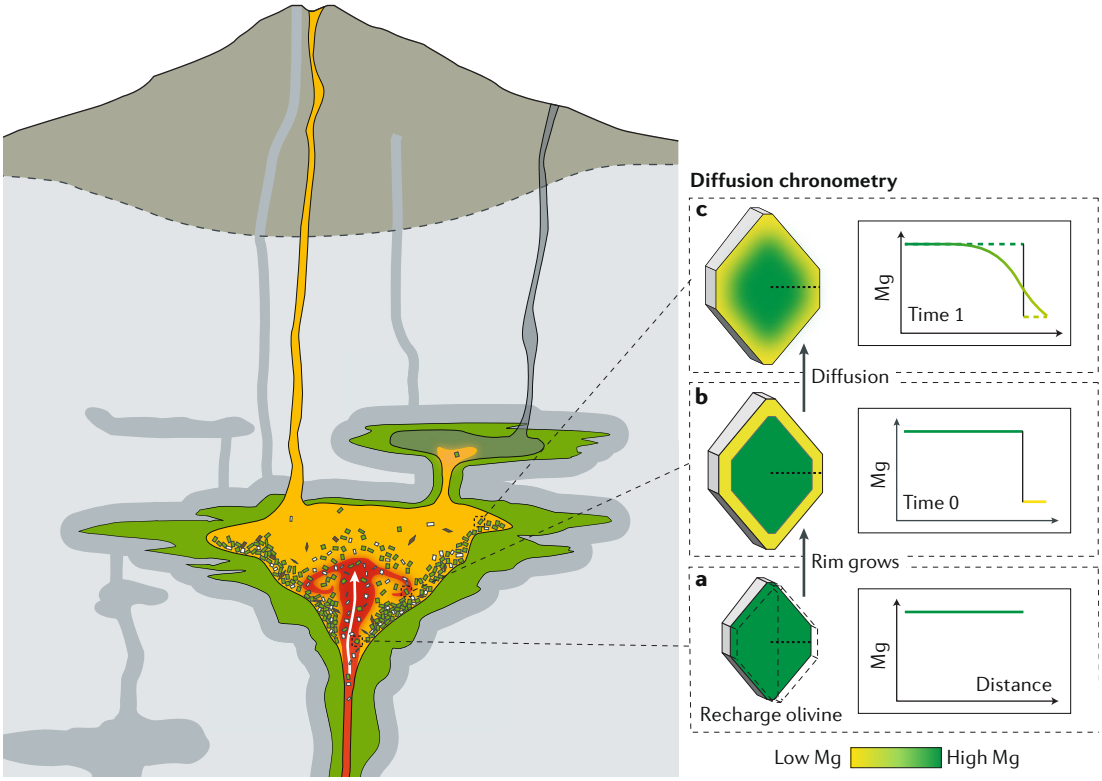

Fig. 1 | **Schematic of a basaltic magma system below a volcano.** A combination of phase equilibria, thermodynamic models and crystal zoning patterns can provide insights into the architecture of sub-volcanic plumbing systems. Diffusion chronometry (modelling the re-equilibration of chemical gradients within crystals) enables the timescales of magma transport through the reservoir(s) (in addition to other magmatic processes that lead up to eruption) to be constrained. The zoning patterns of olivine (illustrated using Mg as proxy) can develop during the interaction of multiple magma batches. The plots show changes in Mg along analytical profiles collected in the olivine at different steps. The initial olivine crystal (panel **a**) is carried by a mafic (high Mg) magma that is injected into a less mafic (lower Mg) magma reservoir (magma recharge event). The olivine grows a lower Mg rim (panel **b**), which is then modified by diffusion through time (panel **c**). If the diffusivity of Mg in olivine is known, petrologists can model diffusive re-equilibration to constrain the time between magma mixing and eruption (where diffusion effectively stops).

in bulk-rocks, mineral separates and zircons enabled greater resolution of the timescales of magmatic processes. Crystallization of minerals with different U-Th-Ra partition coefficients leads to the fractionation of elements in the U-Th-Ra disequilibrium series, resulting in deviation from secular equilibrium and the start of the radiogenic clock[26,27]. Commonly used systems include the decay of ^{238}U to ^{230}Th and ^{230}Th to ^{226}Ra, which have half-lives on the order of 75,000 years and 1,600 years, respectively, as they can access the timescales of processes operating over hundreds to hundreds of thousands of years[30].

The majority of studies that have investigated the use of U-Th-Ra disequilibria in magmatic systems have used zircons to constrain the residence times of large-volume (10–1,000 km^3), silica-rich magma bodies beneath caldera-forming volcanic systems. Timescales derived from zircon ages are relatively long, on the order of tens to hundreds of thousands of years[27,46–48]. Timescales can also be derived from the analysis of Ra-Th isotopic disequilibria in bulk aggregates of feldspar grains[27,28], which return times of several hundred to thousands of years for silica-rich systems (for example, dacites of Mount St Helens volcano)[49]. U-Th-Ra disequilibria series provide absolute crystallization ages for the volcanic crystals under analysis. However, crystal ages are not always easily related to causative processes leading up to eruption and, as multiple grains need to be aggregated to obtain a precise age, uncertainty is introduced by amalgamating crystals and crystal zones with different ages. As a result, it is often difficult to unambiguously interpret the data as a mineral-crystallization age[28]. The issues and uncertainties presented by both mineral-reaction chronometers and the U-Th-Ra decay series highlight the need for new methods that can access short-timescale processes (hours to centuries) and relate the recovered timescales to causative magmatic processes.

Basics of diffusion chronometry

Diffusion chronometry, which uses re-equilibration of chemical disequilibria within volcanic minerals and/or glass to constrain the timescale of magmatic processes, displays several advantages compared with the mineral-reaction chronometers and the U-Th-Ra disequilibria-series approach. For example, chemical re-equilibration can be used to relate timescales to specific, albeit interpretative, magmatic processes and can constrain processes acting on short timescales (hours to days), such as magma ascent prior to eruption.

Partition coefficients
Measures of the preference of a given element to be incorporated in a mineral (compatible) or remain in the melt (incompatible).

Secular equilibrium
Condition where the quantity of a radioactive isotope remains constant.

Half-lives
The time required for half the amount of the parent radioactive isotope to decay into a daughter one; disequilibria can usually be detected for ~5 times the half-life of the daughter.

Chemical zoning patterns preserved in volcanic crystals are a unique record of magmatic processes that can provide insights into the timescales of magmatic processes and, possibly, eruption triggers[23,39,50–52]. Gradients in the composition (and, thus, the chemical potential) of volcanic crystals can result from crystallization, which causes melt differentiation and the development of crystal zonation, or open-system processes such as magma mixing and mingling. The formation of chemical gradients in crystals and/or melts drives the diffusion of molecules or elements during magma storage at high temperatures as the system attempts to return to equilibrium (FIG. 1). If the diffusivities (at magmatic temperatures) of the elements of interest are known[22], the timescale of diffusive re-equilibration can be calculated using Fick's second law of diffusion or more sophisticated models[17,53] (BOX 1). As a result, diffusion chronometry can provide critical information regarding the storage time of crystals at magmatic temperatures[17,53].

Box 1 | **Terms and definitions in Fick's second law**

If gradients in chemical composition are present within a crystal or melt, Fick's second law can be used to obtain the time (*t*) that a crystal spends at a given temperature. Fick's second law, for a single dimension and for a diffusion coefficient (*D*) that is independent of direction in space (*x*) or concentration (*C*), is:

$$\frac{\partial C}{\partial t} = D\frac{\partial^2 C}{\partial x^2}$$

This equation can be solved with numerical methods (such as finite differences) or, in certain cases (see the figure), analytically. One of the most common analytical solutions uses the error function[17,53,109]:

$$C = C_2 + \frac{(C_1 - C_2)}{2} * Erfc\left(\frac{x}{2\sqrt{D * t}}\right)$$

If the initial conditions, boundary conditions and diffusion coefficient of the element of interest are known, the time can be obtained by fitting a model to the concentration profile[43]. Boundary conditions control whether the crystal exchanges matter with its surroundings (open to flux) or not (isolating boundary). The initial condition refers to the shape of the compositional profile before diffusion is considered. The complementary error function (*Erfc*) solution above is for a planar source and infinite media[109]. In this case, the diffusion model can be run for a range of different times and the misfit between the model and the data can be measured at each time interval (using, for example, the mean-square-root method)[110]. Therefore, the misfit at each time step can be used to determine the best model time. Some of the diffusion models can be carried out using user-friendly software[110].

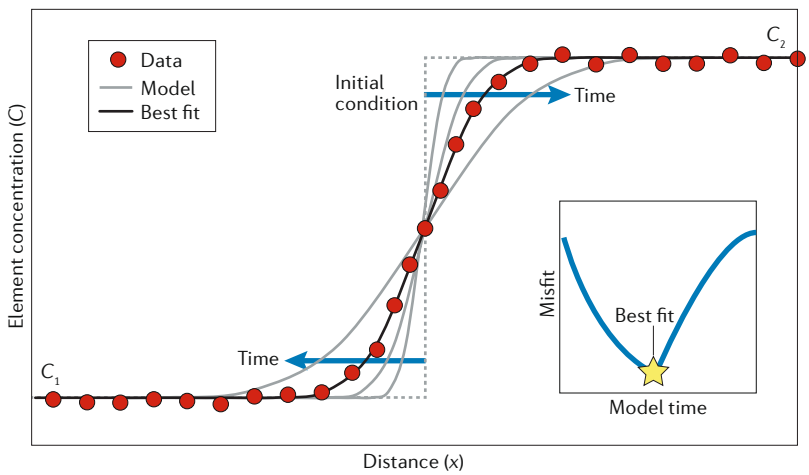

Furthermore, as some elements possess very different diffusivities, it is possible to investigate processes operating over a wide range of timescales, from seconds to hundreds of thousands of years, using diffusion chronometry (FIG. 2).

Measuring chemical zoning patterns

To extract time information from minerals and glass, it is critical to be able to measure their major, trace or isotopic composition with a high level of precision (typically >10 %) and at a high spatial resolution (typically ≤1–5 μm). Huge improvements in the spatial resolution, dimension, precision and speed at which it is possible to determine the in situ elemental, and, in some cases, the isotopic, composition of minerals and glasses enable diffusion chronometry to be applied to a wide range of magmatic processes, utilizing multiple elements with different diffusivities. New developments include the availability of: nanoscale secondary-ion mass spectrometry (NanoSIMS), which can constrain element concentrations at sub-micrometre spatial resolution and parts per million concentration levels[54]; two-dimensional mapping of entire crystals using laser ablation inductively coupled plasma mass spectrometry (FIG. 3), which enables concurrent high-resolution and high-precision analysis of multiple trace elements[24,25,55]; the use of femtosecond lasers, which can be coupled to mass spectrometers to determine zoning of major element isotopes (such as Mg isotopes in olivine)[56]; the atom probe, which can achieve nanometre-scale resolution[57]; and the use of computed tomography scanning to reconstruct zoning in three dimensions[58,59]. Development of other techniques, such as scanning electron microscope imaging and X-ray fluorescence microscopy synchrotron mapping, have improved the sensitivity and speed of analysis, which enable the collection of elemental images for hundreds of crystals[60–62]. Increased analytical capabilities enable access to multiple elements and timescales in a single crystal, as well as in a large population of crystals, and allow diffusion versus crystal-growth zoning models to be tested (see below). Furthermore, analytical developments, alongside new computational methods, enable the random sectioning effect of using petrographic thin sections (taking random 2D planes of 3D crystals), and the representativity of the crystal population, to be assessed[60,63].

Multi-element compositional maps obtained via laser ablation inductively coupled plasma mass spectrometry, especially in minerals like clinopyroxene, exemplify the analytical progress that has been made (FIG. 3). Clinopyroxene incorporates a wide spectrum of major and trace elements with different physical properties, ranging from fast-diffusing, low-charge cations (Li, Ni), to slow-diffusing, high-charge cations (Cr, Zr). The wide range of elemental diffusivities means that multiple elements can be exploited simultaneously to obtain a more accurate picture of the variety of processes and timescales that can be recorded in a single crystal[25,39,50]. In principle, if they record the same process, and the respective diffusion coefficients have been properly calibrated, different elements measured in the same crystal should give comparable diffusion timescales.

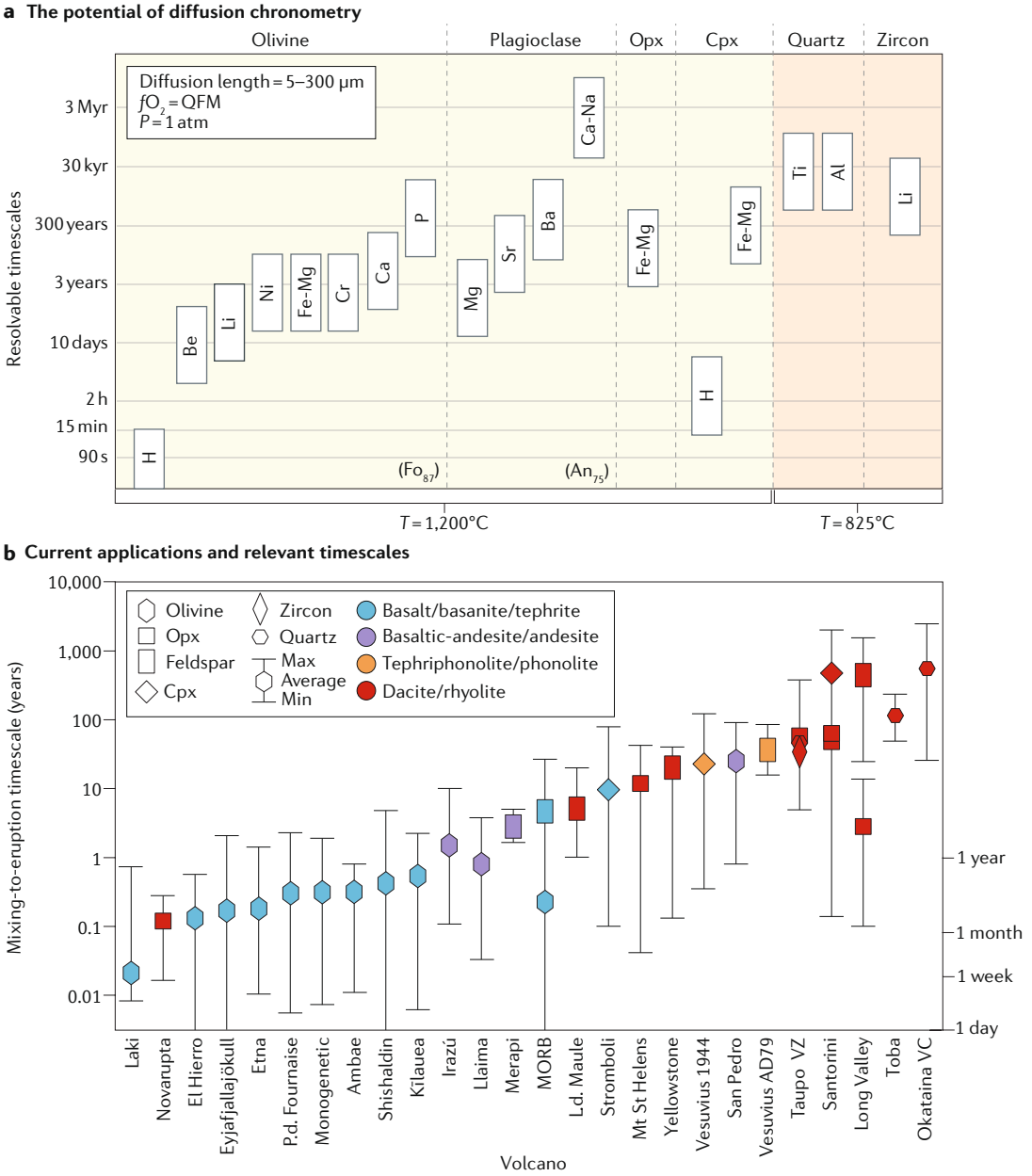

Fig. 2 | **The potential and current applications of diffusion chronometry. a** | The range of timescales that can be obtained from different elements and minerals for a specified temperature (T = 1,200 °C and 825 °C for basalt-hosted and rhyolite-hosted minerals, respectively), pressure (P), oxygen fugacity (fO_2; here, corresponding to the quartz-fayalite-magnetite (QFM) buffer) and diffusion length scales. A wide range of timescales can now be accessed by diffusion chronometry due to the availability of more precise diffusion coefficients and the increased spatial resolution at which chemical gradients can be measured in natural crystals. Diffusion timescales are shown for: H (REF.[111]), Be (REF.[112]), Li (REF.[65]) (slow diffusion mechanism), Ni (REF.[113]), Fe-Mg (REF.[54]), Cr (REF.[114]), Ca (REF.[115]) and P (REF.[116]) in olivine; Mg (REF.[117]), Sr (REF.[118]), Ba (REF.[119]) and Ca-Na (REF.[120]) in plagioclase; Fe-Mg (REF.[121]) in orthopyroxene (Opx); H (REF.[122]) and Fe-Mg (REF.[123]) in clinopyroxene (Cpx); Ti (REF.[124]) and Al (REF.[125]) diffusion in quartz; and Li (REF.[67]) in zircon. **b** | Compilation of mixing-to-eruption timescales that have been obtained for different volcanoes worldwide. Symbols represent different minerals and the symbol position represents the average mixing-to-eruption timescale recorded by that mineral system; symbol colours correspond to magma compositions. Timescales of magma recharge and/or mixing prior to eruption at basaltic volcanoes generally span weeks to a few years, whereas decadal to centennial magma-mixing timescales are more typical of volcanoes erupting more evolved magma. Volcanoes used in this compilation include: Laki[126]; Novarupta[127]; El Hierro[128]; Eyjafjallajökull[82]; Etna[76,83,129,130]; Piton de La Fournaise[131] (P.d. Fournaise); monogenetic eruptions[85,88,132,133]; Ambae[134]; Shishaldin[84]; Kīlauea[77,78]; Irazú[86,135]; Llaima[79]; Merapi[136]; mid-ocean ridge basalt[137–139] (MORB); Laguna del Maule[140] (L.d. Maule); Stromboli[40,141]; Mt St Helens[141]; Yellowstone[54]; Vesuvius[142,143]; San Pedro[144]; Taupo Volcanic Zone[94,145–147] (VZ); Santorini[95,148,149]; Long Valley[96]; Toba[149]; Okataina Volcanic Centre[149] (VC).

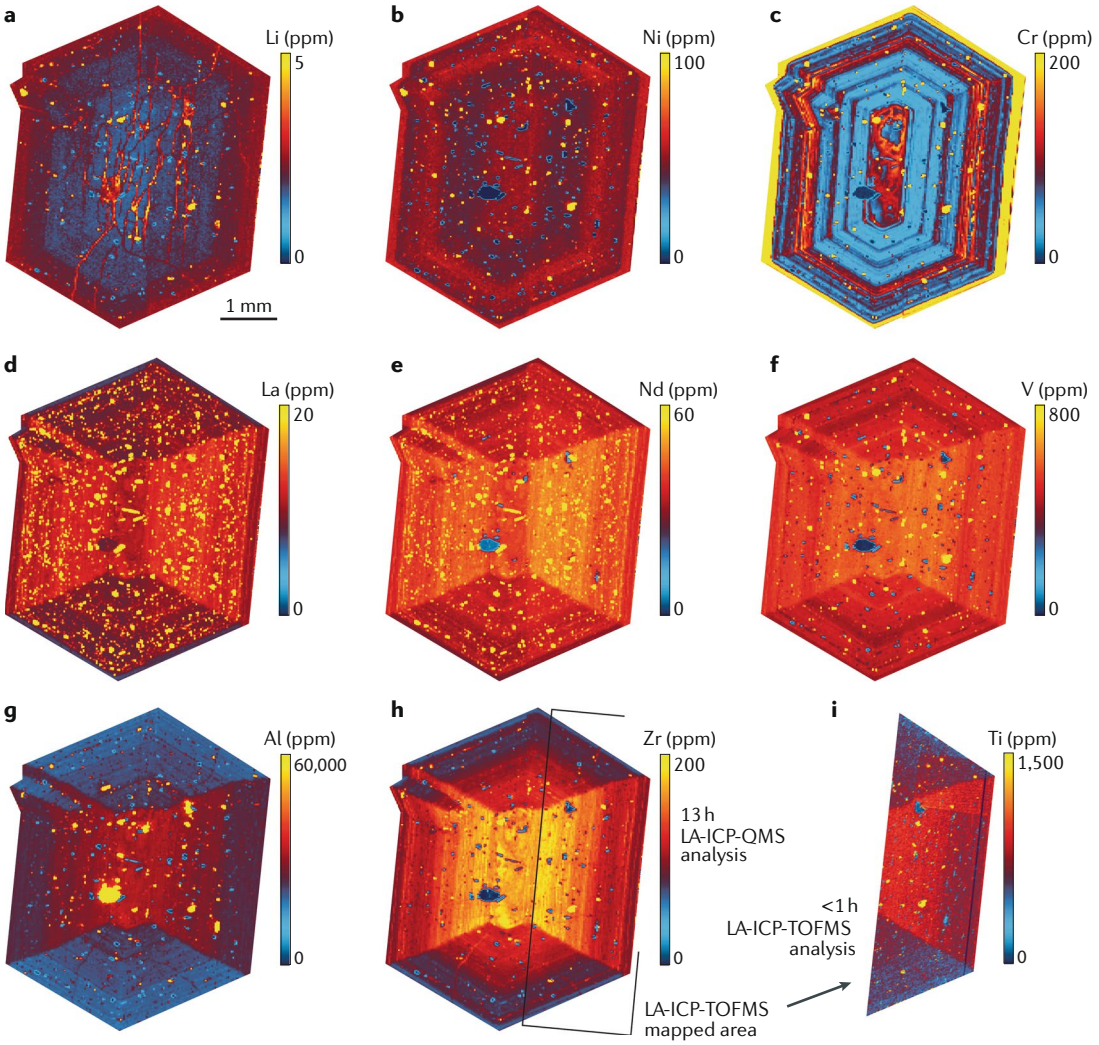

Fig. 3 | **Multi-element chemical map of a clinopyroxene megacryst from Stromboli volcano.** The clinopyroxene megacryst (characterized in REF.[55]) displays a range of zoning patterns, including oscillatory and sector zoning. Low-charge elements (such as Li and Ni) typically show blurred (diffusion-influenced) zoning patterns, whilst high-charge cations (such as Cr and Zr), which diffuse more slowly than low-charge elements in the crystal structure, preserve sharp compositional contrasts that are indicative of protracted processes. Whole-crystal maps were obtained simultaneously in a single, 13-h analytical session with laser ablation inductively coupled plasma quadrupole mass spectrometry (LA-ICP-QMS[24,55]; panels **a**–**h**). A fraction of the crystal (defined by the black box in panel **h**) was then mapped via laser ablation inductively coupled plasma time-of-flight mass spectrometry (LA-ICP-TOFMS)[55], which records full mass spectra (from ^{23}Na to ^{238}U) in comparatively short analytical times (less than 1 h in this example; panel **i**). Adapted from REF.[150], CC-BY-4.0 (https://creativecommons.org/licenses/by/4.0/).

Extracting time from chemical zoning

A key requirement for successful diffusion chronometry is the availability and reliability of diffusion coefficients in silicate systems. Diffusion coefficients are typically experimentally determined and there has been a surge in the number and precision of diffusion coefficients available for most silicate mineral groups[20]. Nevertheless, there are still very limited data sets for minerals such as amphibole, alkali feldspar and biotite. Moreover, variables in addition to temperature, such as pressure, oxygen fugacity, water fugacity and the concentration of impurities, control diffusion coefficients in silicate materials[53]. As a result, there is a need to develop theoretical models that incorporate a more mechanistic and detailed view of how elements diffuse through the crystal lattice. Such models would enable experimental diffusivities to be extrapolated over a wider range of values for all relevant parameters with more confidence[22].

As an example, the diffusion coefficient for the coupled migration of Fe and Mg in olivine ([{Fe,Mg}$_2$SiO$_4$]; D^{Ol}_{Fe-Mg}) is controlled by the concentration and type of point defects that are present, which are mainly dependent on temperature[64]. Nevertheless, other variables, such as pressure, crystallographic orientation, major element composition, oxygen and water fugacity, and the concentration of certain trace elements (such as Fe^{3+}), influence D^{Ol}_{Fe-Mg} (REF.[64]). Therefore, a formulation of D^{Ol}_{Fe-Mg} based on theoretical models that incorporate all of these effects provides a more reliable application to natural systems[53,64]. In addition, there is increasing evidence

Point defects
Defects in the lattice structure of solid media that can represent missing atoms (vacancies) or extra atoms (interstitials).

Anisotropic diffusion
Diffusion coefficients in crystals may vary according to crystallographic axes, owing to the different arrangement of atoms in non-cubic minerals.

Plutonic bodies
Magmatic environments below the Earth's surface (within the crust), where magmas cool slowly and form plutonic rocks, such as granites.

that some elements, especially single-charged cations with small ionic radii, such as H^+ and Li^+ in olivine[65,66] and Li^+ in zircon[67], have multiple diffusion mechanisms. All different diffusion mechanisms must be considered when modelling diffusion in natural crystals.

With knowledge of the diffusion coefficient of the element of interest, as well as the presence of a compositional gradient within a mineral or glass, we can use Fick's second law of diffusion to obtain timescales for a given temperature (BOX 1). For non-ideal systems (such as Mg and Sr in plagioclase, whose partitioning behaviour is dependent on the major-element composition of the crystal)[68,69], more sophisticated equations are required to account for gradients in chemical potential, rather than the measured concentrations. As chemical zoning patterns are typically the combined result of crystal growth and diffusion at a variety of temperatures, the assumption that chemical zonation is the result of diffusion alone is a simplified view of natural systems. However, the importance of diffusion versus growth can be tested in a variety of ways, which include: modelling anisotropic diffusion of elements in two dimensions; modelling diffusion of multiple elements with different diffusivities and crystal-melt-partitioning relationships[70,71]; and integration of magma differentiation and diffusion models[53,71] (see FIG. 4 for an example in olivine). In addition, uncertainties and/or inaccuracies in the initial conditions (BOX 1; the geometry of the initial concentration profile) can result in significant errors in the estimated timescales. Uncertainties in the initial conditions can, however, be overcome by comparing the influence of growth and diffusion on chemical zoning patterns, and specifically through comparing slow-diffusing and fast-diffusing elements in a single crystal[68] (such as using Ba and Sr zoning in sanidine to estimate the initial concentration profile of Mg)[54].

The choice of temperature used in diffusion modelling also has a large influence on the timescales derived from this method, owing to the strong relationship between temperature and the diffusion coefficient for a particular element. For some systems, such as olivine in basalt, the temperature of the system can be calculated using the composition of the crystal of interest, which has been shown to be practical and realistic for most situations[53]. In other cases, it might be possible to account for the large temperature gradients in magmatic systems via calculation of multiple temperatures from mineral-based thermometry (such as clinopyroxene crystals from Stromboli volcano)[40,72]. However, it is difficult to constrain the complex thermal histories of plutonic bodies that have experienced prolonged fluctuations in temperature and composition over time[73]. Moreover, given the errors associated with geothermometers (≥50 °C) and/or phase-equilibria studies (typically <25 °C), the timescales obtained from diffusion chronometry are typically only accurate to about half an order of magnitude[17,53].

The uncertainties outlined above relate to the accuracy with which intrinsic parameters of the natural system (such as temperature and/or the initial concentration profile in zoned crystal) can be estimated. However, there are other, potentially very important, errors associated with the experimental calibration of the diffusion coefficient (such as the activation energy and pre-exponential factor)[53]. Nevertheless, for comparison of results obtained using the same element and mineral, the relative timescales between individual crystals or samples should be accurate. The use of Bayesian statistics can improve the robustness of the time estimates[74].

Despite the seemingly large errors, and the large range of timescales at which various magmatic processes operate, the results from diffusion chronometry

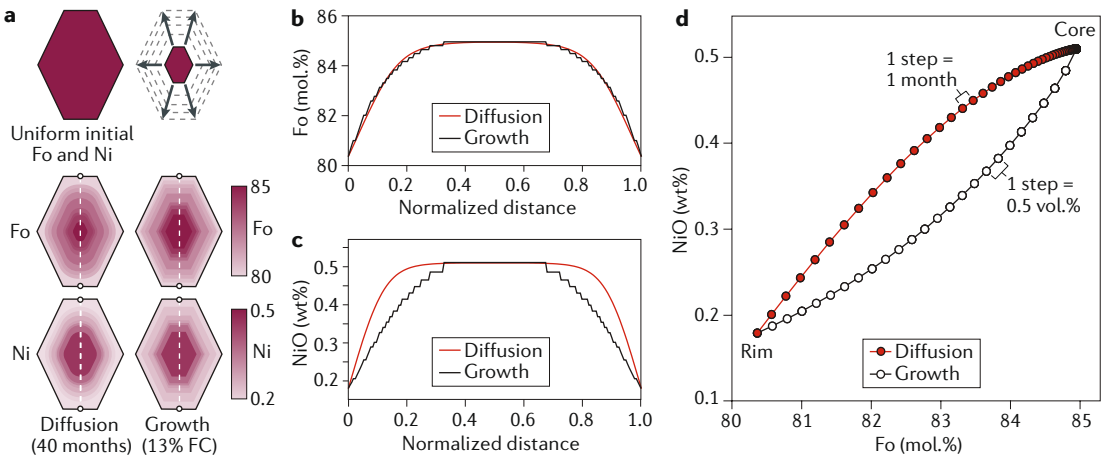

Fig. 4 | **Comparison of the effects of diffusion and crystal growth.** Concentration profiles of Ni and Fo (Mg/[Mg + Fe], using Mg and Fe atoms of per formula unit) can be used to distinguish between growth (13% fractional crystallization (FC)) and diffusion (40 months at 1,200 °C) in olivine phenocrysts. **a** | Concentration gradients obtained after diffusion or growth in modelled crystals are depicted as colour gradients (transects are shown as dashed lines). Note that pure growth zoning preserves sharp concentration contours, while diffusion yields more rounded contours. **b,c** | The zoning patterns that would result from FC and diffusion. Diffusion and growth have very different effects on the NiO zoning that is present. Fo diffuses faster than Ni and shows a gradient that has progressed further towards the core. **d** | On a plot of Fo versus Ni, the diffusion and growth mechanisms create different zoning patterns that can be used to decide whether a given compositional profile in olivine is dominated by growth or diffusion.

Geothermobarometry
Calculation of the pressure and temperature of crystallization using experimentally calibrated models and the composition of natural mineral–glass or mineral–mineral pairs.

Sub-Plinian
Explosive eruption with similar dynamics to Plinian events but of lower intensity and eruptive column height.

provide critical, first-order constraints on the rate of magmatic processes that cannot be obtained by any other method. By combining diffusion chronometry with other petrological and/or geochemical approaches, such as geothermobarometry[75] thermal modelling of magma intrusion and reservoir cooling, and the absolute dating of crystals, we can further constrain the timescales governing the growth and evolution of magmatic systems.

Insights from diffusion chronometry

Diffusion chronometry has been widely applied to volcanic rocks to characterize the timescales of magma storage, mixing and transport towards eruption. In this section, we discuss these applications focusing on two broad topics, magma replenishment and eruption of mafic volcanoes, and the timescales of remobilization of large silicic magma bodies in relation to the timescales derived from dating magmatic zircons.

Mafic magmas and volcano monitoring

Mafic magmas (such as basalt and basaltic andesite) and their associated olivine crystals have been the focus of many diffusion-chronometry studies. Especially, linking normal, reverse and complex zoning of Mg-Fe, Ni, Ca and Mn concentrations in olivine crystals with magma-intrusion events has enabled the time between magma replenishment and transfer of crystals between different magmatic environments to be quantified. Using this method, the timescales of magmatic processes have been investigated in highly active, volcanic systems such as Etna (Italy), Llaima (Chile) and Kīlauea (Hawaii)[76–79]. Olivine has several advantages for diffusion-chronometry studies, including the presence of experimentally characterized diffusion coefficients[80] for major, minor and some trace elements, and the development of theoretical models of point-defect concentrations[64]. Moreover, analytical advances allow the routine high-resolution, and multidimensional, analysis of multiple major and trace elements in olivine crystals[70]. It is, therefore, possible to model the diffusion of multiple elements with different diffusivities in a single crystal, which (among other benefits) enables the relative effects of growth and diffusion to be evaluated[71] (FIG. 4). As a result, olivine has been dubbed the *Drosophila* (that is, the fruit fly that has been key in genetics research) of experimental and natural studies of diffusion in silicates[16].

Diffusion-chronometry studies that have used olivine analysis to focus on active mafic volcanoes typically find short timescales of days to about a decade between magma intrusion (or magma mixing) and transfer between reservoirs before eruption. The estimated timescales are on the same order of magnitude as the eruption frequencies at such volcanoes[81]. It can, therefore, be hypothesized that magma intrusion and magma mixing times revealed by crystal clocks are a robust record of the vigour and steady-state nature of regularly active mafic systems, where most eruptions are driven by frequent intrusion of new magma. We do not, however, have enough data to perform statistically meaningful tests of the relationship between eruption frequency and characteristic magma-replenishment rates. In future, diffusion chronometry, in conjunction with volcanic-monitoring data and/or eruptive frequencies, could provide critical information for deterministic models of eruption forecasting.

Correlation of diffusion chronometry to volcano-monitoring signals. If the date of a volcanic eruption is known, the relative timing of pre-eruptive magmatic processes that are constrained via diffusion chronometry can be recalculated into absolute times. The absolute times can then be converted into a time series of, for example, magma-intrusion events and compared directly with time series of geophysical or geochemical monitoring data (such as seismicity, deformation or changes in the gas chemistry and/or flux)[76,82,83]. Associating temporal information of the magmatic processes documented by crystals with available monitoring data enables causative links between the process happening within a volcano and a given monitoring signal to be identified. Importantly, information obtained from the study of past eruptions can be translated into the assessment of volcanic hazards in the future.

Indeed, a recent study of the 1999 sub-Plinian basaltic eruption from Shishaldin volcano in Alaska successfully correlated volcanic-monitoring signals with timescales derived from diffusion chronometry[84] (FIG. 5). By studying zoning patterns in olivine crystals, three main magma-mixing events were identified. Integration of depths obtained from melt inclusions, seismicity and modelling of Fe-Mg zoning in the olivine revealed that the first mixing event (deep magma

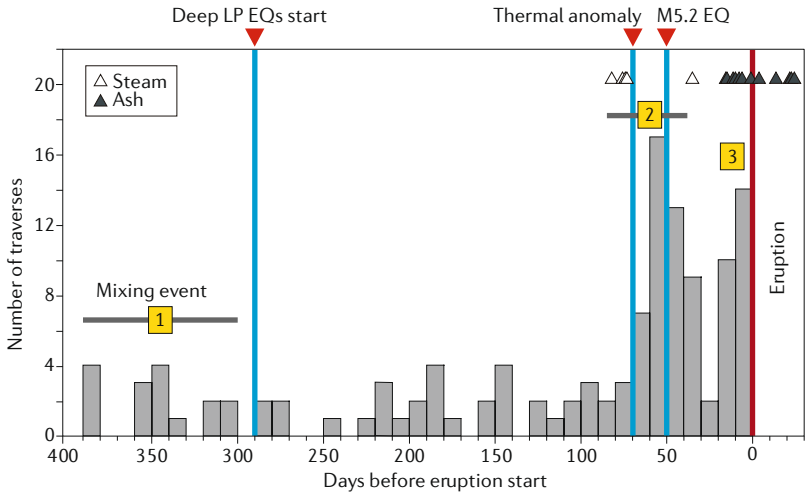

Fig. 5 | **Correlation of diffusion chronometry with monitoring data.** A histogram of timescales obtained from modelling Fe-Mg zoning patterns of olivine from the 1999 mafic explosive eruption of Shishaldin volcano (Alaska). The grey bars represent the time estimates from olivine-based diffusion chronometry, which have been recalculated with regards to the eruption time and, thus, give absolute times. The yellow squares represent the timing of the three most probable mixing events reported in the study in which this histogram was originally reported[84]. Key observations from the monitoring data that relate to the eruption include the onset of deep, long-period (LP) earthquakes (EQs) that may track the arrival of magma at depth (mixing event 1), later followed by the appearance of thermal anomalies and a magnitude 5.2 earthquake (M5.2 EQ) about 2 months before the eruption (corresponding to magma-mixing events 2 and possibly 3). Adapted with permission from REF.[84], Elsevier.

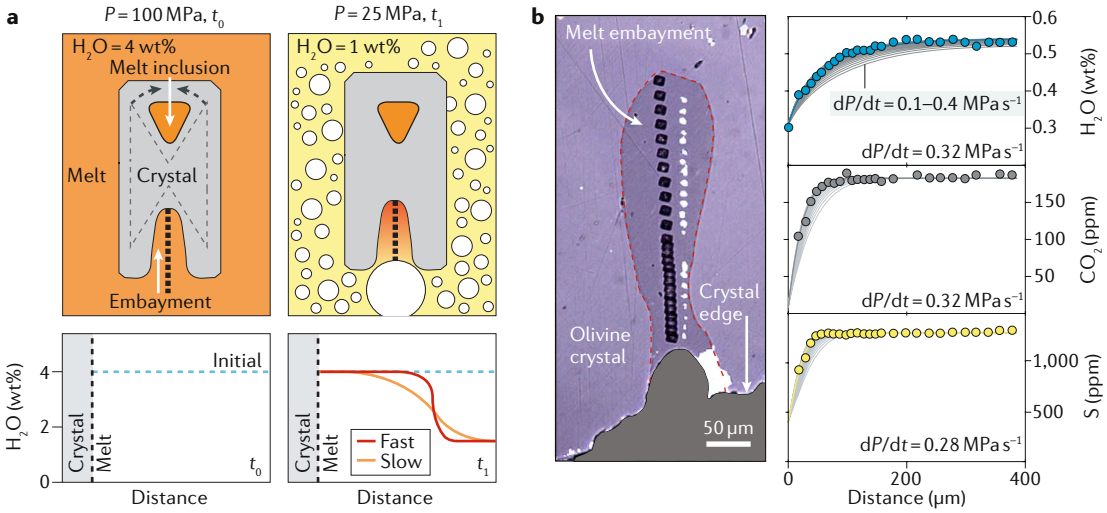

Fig. 6 | **Use of melt embayments to determine timescales of magma decompression. a** | Phenocryst growth can form a melt inclusion or a melt embayment with a volatile content corresponding to the initial volatile content of the external melt (here, 4 wt% H_2O at 100 MPa). During ascent, the outside melt will lose volatiles, owing to degassing. Meanwhile, the embayment lags behind, does not vesiculate and re-equilibrates by diffusion. The red curve shows a concentration gradient measured for fast decompression (short total duration), whereas the orange curve shows the profile expected from slower decompression. **b** | Example of decompression rates extracted by REF.[91] for an olivine embayment within a Hawaiian basalt. The correspondence in decompression rates obtained from several volatiles (H_2O, CO_2 and S) with different diffusivities helps to confirm that the result is robust. Part **b** adapted from REF.[91], Springer Nature Limited.

interactions at ~20-km depth) occurred as early as ~300 days before eruption, coinciding with the onset of long-period earthquakes. The next magma-mixing event occurred ~60–50 days before eruption, after a thermal anomaly and preceding a regional earthquake of M5.2 that was associated with volcano tectonic swarms <7 km below the summit crater. The last mixing event happened alongside the start of the eruption, suggesting that the eruption itself induced mixing, an observation that had previously been made on Etna[67]. Furthermore, the progressive shallowing of magma interactions towards the surface (revealed by volcanic seismicity) was matched by the calculated entrapment depths of the olivine-hosted melt inclusions. Therefore, diffusion chronometry, together with monitoring data, provides a robust and integrated method for understanding the progressive movement of magma towards the surface and eruption. A similar time–depth evolution of magma towards the surface was also recorded at Llaima volcano (Chile)[79]. Further studies integrating diffusion chronometry with volcanic-monitoring data could inform conceptual models of the lead-up to eruption that will aid future risk mitigation from volcanic hazards.

Timescales and processes in dormant and poorly monitored volcanoes. Diffusion chronometry also provides important information on volcanic systems for which no monitoring data exist. For example, the application of diffusion chronometry, combined with petrological observations and barometric estimates, to prior eruptions from monogenetic volcanic fields[85,86] is critical because both the location and the timing of monogenetic eruptions are hard to forecast[87]. Analysis of major-element and minor-element zoning in olivine crystals from past monogenetic eruptions reveal magma mixing and mobilization on timescales that range from years to months prior to eruption; however, the final ascent of magma to the surface from the last reservoir might be notably shorter than this timescale[85,88].

To investigate magma-ascent rates, several studies have focused on the zoning of fast-diffusing volatile elements (such as H and Li) in minerals or melt embayments. As magmas ascend, volatiles (such as H_2O, CO_2 and S) that were dissolved within the ascending magma become insoluble and exsolve into a separate vapour phase. Volatile exsolution creates a large chemical gradient between the ascending magma and the composition of crystals and melt embayments formed at higher pressures within the volcanic plumbing system (FIG. 6). The chemical gradient that is generated drives diffusion of volatile species into the carrier melt and/or vapour phase, resulting in the loss of volatiles from the crystals and melt embayments. As volatiles migrate from the interior of the crystal or embayment to the outside melt, concentration gradients are generated, which can be leveraged to extract timescale information through diffusion chronometry (FIG. 6). Identification and modelling of H zoning in phenocrystic or xenocrystic olivine hosted in mafic magmas[89,90] (from Pali-Aike, Chile, and Cerro Negro, Nicaragua) return magma-decompression rates on the order of 0.01–0.1 MPa s^{-1}. In addition, magma-ascent and/or magma-decompression rates derived from modelling H_2O, CO_2 and S diffusion in olivine-hosted embayments from Kīlauea volcano yield a comparable range of decompression rates[91], between 0.05 and 0.5 MPa s^{-1} (FIG. 6).

In summary, quantification of the characteristic timescales between magma intrusion, transport and eruption at undermonitored or dormant volcanoes

Monogenetic volcanic fields
Areas in which volcanoes are built by a single eruption. They are typically small cones of a few tens to a few hundred metres tall, basaltic in composition and formed over time frames of weeks to years.

provides important information for potential hazard-management efforts. As a result, diffusion chronometry can identify the time frame available for emergency planners to prepare for an upcoming eruption or for the reawakening of a given volcano.

Ages and diffusion in silica-rich magma

Large-volume (10–1,000 km^3), explosive, dacitic-to-rhyolitic eruptions from caldera-forming systems have been widely studied, owing to their influence on climate and evolutionary biology[92]. Diffusion chronometry, in combination with other techniques such as U-Th dating of magmatic zircons, has the potential to address several key challenges associated with the generation of large silicic eruptions, including the rate at which such large amounts of melt can be generated and how fast can it be remobilized prior to eruption[93]. Answering these questions is also critical for understanding the rate of formation of the Earth's crust.

The diverse mineralogy of most silicic systems enables diffusion chronometry to be applied to a range of minerals and elements, including: Ba, Sr and Mg in plagioclase; Ba and Sr in sanidine; Ti in quartz; and Fe-Mg in pyroxenes. Typically, most studies have focused on the rims of the crystals and report timescales that range from a few decades to a few hundred years[54,73,94,95] (FIG. 2b). Importantly, a few studies have combined results from multiple elements in different minerals to obtain several independent timescale estimates. For example, in one study, the zoning patterns of Ba-Sr in sanidine, Ti in quartz and Fe-Mg in orthopyroxene from the Bishop Tuff were investigated[96]. It is found that timescales were in the ranges 1–10 years for Fe-Mg in orthopyroxene, 10–100 years for Ti in quartz and 100–1,000 years for Ba-Sr in sanidine (FIG. 7). Interestingly, the timescales derived from multiple elements and/or minerals are commonly anticorrelated with their diffusivities (such that fast-diffusing elements record shorter timescales), which might provide insights into the cause of the discrepancy between the calculated timescales. For example, in a scenario where a magmatic system experiences several periods of magma recharge and/or heating, slow-diffusing elements might record the accumulated time of all events. Fast-diffusing elements, on the other hand, might re-equilibrate following each event and, thus, only record the final thermal or chemical perturbation to the system prior to eruption. Nevertheless, the origin of the different timescales remains far from certain, and it is unclear whether the wide range of estimated timescales is simply related to uncertainties in the diffusion coefficient of each element. Regardless, the timescales derived from this approach imply that the 600 km^3 of magma that formed the Bishop Tuff was remobilized within a few decades to millennia prior to eruption.

Similarly to olivine-hosted melt embayments in mafic systems, magma-decompression rates can be obtained for explosive silicic eruptions by modelling H_2O diffusion in quartz-hosted embayments (FIG. 6). Diffusion-based decompression-rate estimates from rhyolites that fed large explosive eruptions at Yellowstone (USA), Long Valley (USA) and Taupo (New Zealand) calderas range between 0.01 and 0.1 MPa s^{-1} (REFS[97,98]). The decompression rates estimated via volatile diffusion in melt embayments are typically an order of magnitude lower than those estimated by comparing bubble-nucleation models with the measured number of vesicles in natural pyroclasts (0.1–10 MPa s^{-1} (REFS[35,38])). The discrepancy between the two methods could be related to the non-linearity of magma-ascent rates from depth to the surface: melt embayments might provide a more robust

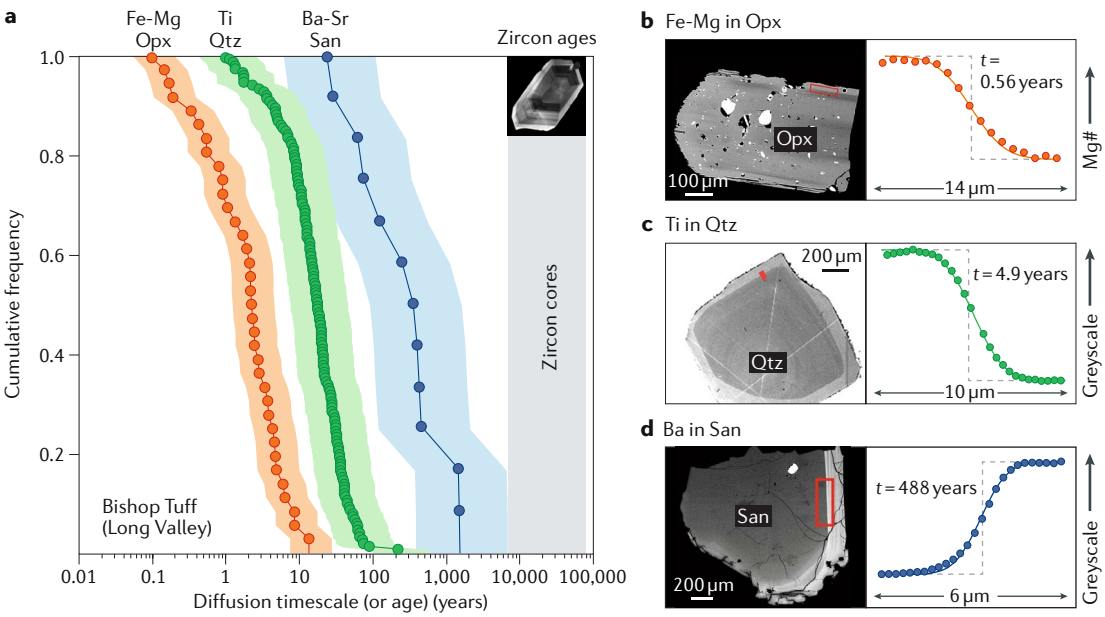

Fig. 7 | **Diffusion timescales obtained from different minerals in silicic systems. a** | A summary of diffusion timescales obtained from the minerals sanidine (San), quartz (Qtz) and orthopyroxene (Opx) found in the high-silica rhyolite of the Bishop Tuff is shown. **b–d** | Examples of the chemical profiles and the best-fit diffusion models for each mineral. Note that the diffusion timescales are relatively short (mostly years to hundreds of years). By contrast, the ages from U-Th dating of zircon are tens to hundreds of thousands of years older. Adapted from REF.[96], Springer Nature Limited.

record of the slower initial ascent and degassing, with bubble textures preserving the last moments of accelerating decompression shortly prior to fragmentation[38]. Therefore, diffusion chronometry can provide insights into the timescales of magma mobilization, and final magma ascent, prior to large silicic eruptions.

In addition, radiogenic dating of magmatic zircons has been used to study the same deposits that were studied by diffusion chronometry[96,99,100], and the results indicate that the zircons are typically several hundreds of thousands of years old. The difference in the timescales derived from diffusion chronometry and radiogenic dating of magmatic zircons could, in part, result from the use of different crystals for each method. However, a recent study[94] applied both techniques to the same zircon crystals and still found that U-Th disequilibria gave much longer timescales (tens of thousands of years) than diffusion chronometry. As a result, the two timescales are likely to track different processes within large silicic systems, and it is necessary to consider what these processes might be.

Several interpretations have been put forward, in the Bishop Tuff and in other large, silica-rich systems, to explain the difference in recorded timescales. One possible interpretation is that diffusion chronometry tracks the time of the last event to perturb the system, such as magma remobilization and/or replenishment shortly prior to eruption, whereas U-Th ages in zircon track the time needed for magma to accumulate[101,102]. However, since diffusion is temperature-dependent, the concentration gradients in the crystals might remain frozen during prolonged residence close to the solidus temperature, where diffusion is markedly slower than at eruptive temperatures and the diffusion clock effectively stops[73]. As a result, diffusion chronometry only tracks the time spent at higher temperature and the diffusion timescales, which are calculated at eruption temperature, might underestimate the total amount of time that the crystals are present in a magmatic environment. By contrast, zircon ages are not sensitive to temperature fluctuations (unless the crystal dissolves) and likely provide a more robust measure of the total residence time of the crystals in magmatic systems. The interpretation presented above is commonly referred to as 'cold storage'[73], but it is not universally accepted. For the same data sets, several authors have also suggested a 'hot-storage' model[103], where magma is stored at high temperatures during most of the prolonged (>100,000 years) magma system history before eruption[104] (see discussion in REF.[105]). Nevertheless, the discrepancy between the times recorded by diffusion chronometry and the times recorded by U-Th series in zircons likely reflects thermal fluctuations experienced by the magma reservoir. Given the large volumes of magma that may be present in these sub-volcanic systems, crystals are likely to have experienced complex thermal histories that are difficult to deconvolve by diffusion chronometry alone.

Zircon is less susceptible than most other silicates to dissolution and reprecipitation during changes to the temperature and/or composition of the system[106]. Hence, zircons can be retained within the same system throughout several episodes of recharge and magmatism, and, thus, record ancient information with respect to the formation and growth of large silicic systems over tens to hundreds of thousands of years, rather than information on the eruption that carried the crystal to the surface. As a result, zircon-crystallization ages have far-reaching implications for the timescales that are required to accumulate large silicic magma bodies in the shallow crust prior to eruption. However, despite the large number of geophysical and tomography studies that have been carried out on silicic volcanoes, shallow accumulation of large silicic magma reservoirs has only been documented in a small number of cases (such as Laguna del Maule[107] in Chile and Uturuncu[108] in Bolivia). Therefore, it is possible that, although magma storage lasts for tens of thousands of years, remobilization and melting of crystal-rich magmas, and the transfer of melts to shallow reservoirs, happens very quickly (within a few decades prior to eruption)[95]. Placing accurate and robust constraints on the duration of storage of large silicic magma bodies at shallow depths within the crust has implications for volcanic monitoring and hazard assessments associated with large explosive eruptions. In particular, it is crucial to understand whether the detection of shallow magma bodies via geophysical and/or tomographic methods indicates that an eruption may be imminent.

Summary and future perspectives

Diffusion chronometry can provide important constraints on the timescales of magmatic processes that precede an eruption. However, its application to a wide range of magmatic processes depends on the availability of accurate and precise diffusion coefficients for the elements of interest. Recent experimental studies have increased the availability and precision of diffusion coefficients relevant to magmatic processes (such as Fe-Mg in olivine). Nevertheless, few data sets incorporate the influence of oxygen fugacity, water fugacity and point defects on element diffusivities. Additional experiments and theoretical models that address the influence of different variables (such as oxygen fugacity) on the concentration of point defects, and, therefore, on the diffusivity of the element and mineral in question, are thus required. Nonetheless, in situations where the diffusion coefficient of the element of interest is well known, recent advances in the spatial resolution and precision of elemental and isotopic analyses in minerals and glass allows the timescales of a wide range of magmatic processes to be estimated.

In mafic systems, the timescales derived from diffusion chronometry (using olivine crystals) from well-monitored eruptions can be correlated with volcanic-monitoring data, including seismicity and deformation. Correlation of the various data streams is encouraging for future applications of diffusion chronometry and enables the construction of more detailed models of the processes that occur beneath volcanoes prior to eruption. However, more work is required to utilize such information in eruption-forecasting models. Specifically, there is typically a disconnect between the crystals used to obtain diffusion timescales and those used to establish magma-storage depths (via geothermobarometry or melt-inclusion-entrapment pressures),

which must be overcome to allow better integration of diffusion chronometry with monitoring data.

Only a limited number of studies have applied diffusion chronometry to multiple minerals and elements from the same sample. In such studies, the timescales extracted from each mineral and/or element are often markedly different (FIG. 7). Typically, there tends to be a negative correlation between the timescales obtained and the diffusion rate of the element under consideration (such that slower-diffusing elements provide longer timescale estimates). Although this variation could indicate discrepancies in the calibrations of the different diffusion coefficients, it is also possible that it could reflect a limitation of the diffusion approach for long-lived systems that undergo complex thermal and compositional fluctuations. For example, fast-diffusing elements might re-equilibrate multiple times, and we are only able to recover the last disequilibrium event, whereas slow-diffusing elements might record a longer, more protracted, history of the magmatic system. Advanced models that link fluid dynamics, thermal evolution of magma reservoirs and acquisition of multi-element data sets at the crystal scale might be able to address the uncertainties outlined here.

Finally, there is a large discrepancy between the timescales recorded by diffusion chronometry and U-Th disequilibria dating in magmatic zircons from large silicic eruptions. Although timescales from diffusion chronometry and U-Th disequilibria can be obtained in a single zircon, it is puzzling why diffusion chronometry records shorter timescales than U-Th disequilibria. The thermal history of the magma reservoir is one of the key factors that might help to explain this discrepancy. It is unclear if most crystals are stored at temperatures close to the solidus before eruption, so that the diffusion clock basically stops, or if they crystallize immediately before eruption. Combining new data sets (including diffusion-chronometry and zircon-dating approaches) with detailed thermal models of magma reservoirs will provide a more detailed image of the growth and amalgamation of large silicic magma bodies within the crust. Thus, combining diffusion chronometry with other techniques could help to interpret geophysical images of magma reservoirs in the shallow crust and contribute to a better assessment of volcanic hazards.

Published online: 01 April 2020

1. Bowen, N. L. *The Evolution of the Igneous Rocks* (Princeton Univ. Press, 1928).
2. Young, D. A. *Mind Over Magma: The Story of Igneous Petrology* (Princeton Univ. Press, 2003).
3. Pichavant, M. et al. Equilibration scales in silicic to intermediate magmas-implications for experimental studies. *J. Petrol.* **48**, 1955–1972 (2007).
4. Ghiorso, M. & Sack, O. Chemical mass transfer in magmatic processes IV. A revised and internally consistent thermodynamic model for the interpolation and extrapolation of liquid-solid equilibria in magmatic systems at elevated temperatures and pressures. *Contrib. Mineral. Petrol.* **119**, 197–212 (1995).
5. Blundy, J. & Cashman, K. Petrologic reconstruction of magmatic system variables and processes. *Rev. Min. Geochem.* **69**, 179–239 (2008).
6. Cashman, K. V., Sparks, R. S. J. & Blundy, J. D. Vertically extensive and unstable magmatic systems: A unified view of igneous processes. *Science* **355**, eaag3055 (2017).
7. Caricchi, L. et al. Non-Newtonian rheology of crystal-bearing magmas and implications for magma ascent dynamics. *Earth Planet. Sci. Lett.* **264**, 402–419 (2007).
8. Laumonier, M. et al. On the conditions of magma mixing and its bearing on andesite production in the crust. *Nat. Commun.* **5**, 5607 (2014).
9. Ruprecht, P., Bergantz, G. W. & Dufek, J. Modeling of gas-driven magmatic overturn: tracking of phenocryst dispersal and gathering during magma mixing. *Geochem. Geophys. Geosyt.* **9**, Q07017 (2008).
10. Bergantz, G. W., Schleicher, J. M. & Burgisser, A. Open-system dynamics and mixing in magma mushes. *Nat. Geosci.* **8**, 793–796 (2015).
11. Huber, C., Bachmann, O. & Dufek, J. Thermo-mechanical reactivation of locked crystal mushes: melting-induced internal fracturing and assimilation processes in magmas. *Earth Planet. Sci. Lett.* **304**, 443–454 (2011).
12. Annen, C., Blundy, J. D., Leuthold, J. & Sparks, R. S. Construction and evolution of igneous bodies: towards an integrated perspective of crustal magmatism. *Lithos* **230**, 206–221 (2015).
13. Ganguly, J. in *EMU Notes in Mineralogy, Energy Modelling in Minerals* Vol. **4** (ed. Gramaccioli, C. M.) 271–309 (Eotvos Univ. Press, 2002).
14. Lasaga, A. C. in *Princeton Series in Geochemistry* Vol. 402 (Princeton Univ. Press, 2014).
15. Zhang, Y. *Geochemical Kinetics* (Princeton Univ. Press, 2008).
A comprehensive primer of kinetics in earth sciences and a good starting place for anyone wanting to get an introduction on constitutive equations and solutions for diffusion in minerals and melts.
16. Chakraborty, S. Diffusion in solid silicates: a tool to track timescales of processes comes of age. *Annu. Rev. Earth Planet. Sci.* **36**, 153–190 (2008).
17. Costa, F. & Morgan, D. in *Timescales of Magmatic Processes: From Core to Atmosphere* (eds Dosseto, A., Turner, S. P. & Van Orman, J. A.) 125–159 (Wiley, 2010).
18. Wood, J. A. The cooling rates and parent planets of several iron meteorites. *Icarus* **3**, 429–459 (1964).
19. Lasaga A. C. in *Kinetics and Equilibrium in Mineral Reactions. Advances in Physical Geochemistry* Vol. 3 (ed. Saxena, S. K.) 81–114 (Springer, 1983).
Sets the foundation of the diffusion-speedometry approach with a mathematical derivation of the equations.
20. Maaløe, S. & Hansen, B. Olivine phenocrysts of Hawaiian olivine tholeiite and oceanite. *Contrib. Mineral. Petrol.* **81**, 203–211 (1982).
One of the first papers that modelled zoning profiles of olivine to extract timescales.
21. Lasaga, A. C., Richardson, S. M. & Holland, H. D. in *Energetics of Geological Processes* (eds Saxena, S. K., Bhattacharji, S., Annersten, H. & Stephansson, O.) 353–388 (Springer, 1977).
22. Zhang, Y. & Cherniak, D. J. Diffusion in minerals and melts. *Rev. Mineral. Geochem.* **72**, 1–4 (2010).
Contains the most recent compilation of experimentally determined diffusion data plus theoretical models of diffusion in melts and crystals.
23. Davidson, J. P., Morgan, D. J., Charlier, B. L. A., Harlou, R. & Hora, J. M. Microsampling and isotopic analysis of igneous rocks: implications for the study of magmatic systems. *Ann. Rev. Earth Planet. Sci.* **35**, 273–311 (2007).
24. Ubide, T., McKenna, C. A., Chew, D. M. & Kamber, B. S. High-resolution LA-ICP-MS trace element mapping of igneous minerals: in search of magma histories. *Chem. Geol.* **409**, 157–168 (2015).
25. Ubide, T., Mollo, S., Zhao, J.-X., Nazzari, M. & Scarlato, P. Sector-zoned clinopyroxene as a recorder of magma history, eruption triggers, and ascent rates. *Geochim. Cosmochim. Acta* **251**, 265–283 (2019).
26. Condomines, M., Gauthier, P. J. & Sigmarsson, O. Timescales of magma chamber processes and dating of young volcanic rocks. *Rev. Mineral. Geochem.* **52**, 125–174 (2003).
27. Cooper, K. M. & Reid, M. R. Uranium-series crystal ages. *Rev. Mineral. Geochem.* **69**, 479–544 (2008).
28. Cooper, K. M. Time scales and temperatures of crystal storage in magma reservoirs: implications for magma reservoir dynamics. *Philos. Trans. R. Soc. A Math. Phys. Eng. Sci.* **377**, 20180009 (2019).
Contains a very detailed compilation of timescales obtained from diffusion chronometry and U-Th dating, and a discussion of the hot and cold magma-storage hypothesis.
29. Ivanovich, M., & Harmon, R. S. *Uranium-Series Disequilibrium: Applications to Earth, Marine, and Environmental Sciences* 2nd edn (Clarendon Press, 1992).
30. Bourdon, B., Henderson, G. M., Lundstrom, C. C. & Turner, S. P. Introduction to U-series geochemistry. *Rev. Mineral. Geochem.* **52**, 1–22 (2003).
31. Putirka, K. D. Minerals, inclusions and volcanic processes. *Rev. Mineral. Geochem.* **69**, 1–8 (2008).
32. Shea, T. & Hammer, J. E. Kinetics of cooling- and decompression-induced crystallization in hydrous mafic-intermediate magmas. *J. Volcanol. Geotherm. Res.* **260**, 127–145 (2013).
33. Hammer, J. E. Experimental studies of the kinetics and energetics of magma crystallization. *Rev. Mineral. Geochem.* **69**, 9–59 (2008).
34. Vona, A. & Romano, C. The effects of undercooling and deformation rates on the crystallization kinetics of Stromboli and Etna basalts. *Contrib. Mineral. Petrol.* **166**, 491–509 (2013).
35. Toramaru, A. BND (bubble number density) decompression rate meter for explosive volcanic eruptions. *J. Volcanol. Geotherm. Res.* **154**, 303–316 (2006).
36. Mangan, M. & Sisson, T. Delayed, disequilibrium degassing in rhyolite magma: decompression experiments and implications for explosive volcanism. *Earth Planet. Sci. Lett.* **183**, 441–455 (2000).
37. Fiege, A. & Cichy, S. B. Experimental constraints on bubble formation and growth during magma ascent: a review. *Am. Mineral.* **100**, 2426–2442 (2015).
38. Shea, T. Bubble nucleation in magmas: a dominantly heterogeneous process? *J. Volcanol. Geotherm. Res.* **343**, 155–170 (2017).
39. Ubide, T. & Kamber, B. S. Volcanic crystals as time capsules of eruption history. *Nat. Commun.* **9**, 326–326 (2018).
40. Petrone, C. M., Braschi, E., Francalanci, L., Casalini, M. & Tommasini, S. Rapid mixing and short storage timescale in the magma dynamics of a steady-state volcano. *Earth Planet. Sci. Lett.* **492**, 206–221 (2018).
41. Allen, J. C. & Boettcher, A. L. The stability of amphibole in andesite and basalt at high pressures. *Am. Mineral.* **68**, 307–314 (1983).
42. Rutherford, M. J. & Hill, P. M. Magma ascent rates from amphibole breakdown: an experimental study applied to the 1980–1986 Mount St. Helens eruptions. *J. Geophys. Res. Solid Earth* **98**, 19667–19685 (1993).
43. Browne, B. L. & Gardner, J. E. The influence of magma ascent path on the texture, mineralogy, and formation of Hornblende reaction rims. *Earth Planet. Sci. Lett.* **246**, 161–176 (2006).

44. Rutherford, M. J. & Devine, J. D. Magmatic conditions and magma ascent as indicated by hornblende phase equilibria and reactions in the 1995–2002 Soufriere Hills magma. *J. Petrol.* **44**, 1433–1453 (2003).
45. Faure, G. & Mensing, T. M. Isotopes: principles and applications 3rd edn. (Wiley, 2005).
46. Cooper, K. M. Timescales of crustal magma reservoir processes: insights from U-series crystal ages. *Geol. Soc. Lond. Spec. Publ.* **422**, 141–174 (2015).
47. Reid, M. in *Treatise on Geochemistry, The Crust* Vol 3. (ed. Rudnick R. L.) 167–193 (Elsevier, 2004).
48. Schmitt, A. K. Uranium series accessory crystal dating of magmatic processes. *Annu. Rev. Earth Planet. Sci.* **39**, 321–349 (2011).
49. Cooper, K. M. & Reid, M. R. Re-examination of crystal ages in recent Mount St. Helens lavas: implications for magma reservoir processes. *Earth Planet. Sci. Lett.* **213**, 149–167 (2003).
50. Costa, F. & Dungan, M. Short time scales of magmatic assimilation from diffusion modeling of multiple elements in olivine. *Geology* **33**, 837–840 (2005).
51. Ginibre, C., Wörner, G. & Kronz, A. Crystal zoning as an archive for magmatic evolution. *Elements* **3**, 261–266 (2007).
52. Streck, M. J. Mineral textures and zoning as evidence for open system processes. *Rev. Mineral. Geochem.* **69**, 595–622 (2008).
53. Costa, F., Dohmen, R. & Chakraborty, S. Time scales of magmatic processes from modeling the zoning patterns of crystals. *Rev. Mineral. Geochem.* **69**, 545–594 (2008).
Provides a detailed methodology to apply the diffusion-chronometry approach, including best practices, as well as finite-difference solutions to the diffusion equation and an explanation of the theoretical models of point defects in olivine.
54. Till, C. B., Vazquez, J. A. & Boyce, J. W. Months between rejuvenation and volcanic eruption at Yellowstone caldera, Wyoming. *Geology* **43**, 695–698 (2015).
55. Ubide, T. et al. Deep magma storage revealed by multi-method elemental mapping of clinopyroxene megacrysts at Stromboli volcano. *Front. Earth Sci.* **7**, 239 (2019).
56. Oeser, M., Dohmen, R., Horn, I., Schuth, S. & Weyer, S. Processes and time scales of magmatic evolution as revealed by Fe–Mg chemical and isotopic zoning in natural olivines. *Geochim. Cosmochim. Acta* **154**, 130–150 (2015).
57. Cao, M. et al. Micro- and nano-scale textural and compositional zonation in plagioclase at the Black Mountain porphyry Cu deposit: implications for magmatic processes. *Am. Mineral.* **104**, 391–402 (2019).
58. Pankhurst, M. J. et al. Monitoring the magmas fuelling volcanic eruptions in near-real-time using X-ray micro-computed tomography. *J. Petrol.* **55**, 671–684 (2014).
59. Moussallam, Y. et al. Megacrystals track magma convection between reservoir and surface. *Earth Planet. Sci. Lett.* **413**, 1–12 (2015).
60. Cheng, L., Costa, F. & Carniel, R. Unraveling the presence of multiple plagioclase populations and identification of representative two-dimensional sections using a statistical and numerical approach. *Am. Mineral.* **102**, 1894–1905 (2017).
61. Zeng, L., Cheng, L., Costa, F. & Herrin, J. CEmin: a MATLAB-based software for computational phenocryst extraction and statistical petrology. *Geochem. Geophys. Geosyt.* **19**, 1378–1392 (2018).
62. Barnes, S. J. et al. Imaging trace-element zoning in pyroxenes using synchrotron XRF mapping with the Maia detector array: benefit of low-incident energy. *Am. Mineral.* **105**, 136–140 (2020).
63. Shea, T., Costa, F., Krimer, D. & Hammer, J. E. Accuracy of timescales retrieved from diffusion modeling in olivine: a 3D perspective. *Am. Mineral.* **100**, 2026–2042 (2015).
64. Dohmen, R. & Chakraborty, S. Fe–Mg diffusion in olivine II: point defect chemistry, change of diffusion mechanisms and a model for calculation of diffusion coefficients in natural olivine. *Phys. Chem. Min.* **34**, 409–430 (2007).
A comprehensive analysis of experimental data and the thermodynamics of point defects in silicates, providing. insight into the variables that play a role in diffusion in olivine.
65. Dohmen, R., Kasemann, S. A., Coogan, L. & Chakraborty, S. Diffusion of Li in olivine. Part I: experimental observations and a multi species diffusion model. *Geochim. Cosmochim. Acta* **74**, 274–292 (2010).
66. Ferriss, E., Plank, T., Newcombe, M., Walker, D. & Hauri, E. Rates of dehydration of olivines from San Carlos and Kilauea Iki. *Geochim. Cosmochim. Acta* **242**, 165–190 (2018).
67. Trail, D. et al. Li zoning in zircon as a potential geospeedometer and peak temperature indicator. *Contrib. Mineral. Petrol.* **171**, 25 (2016).
68. Costa, F., Chakraborty, S. & Dohmen, R. Diffusion coupling between trace and major elements and a model for calculation of magma residence times using plagioclase. *Geochim. Cosmochim. Acta* **67**, 2189–2200 (2003).
69. Zellmer, G. F., Blake, S., Vance, D., Hawkesworth, C. & Turner, S. Plagioclase residence times at two island arc volcanoes (Kameni Islands, Santorini, and Soufriere, St. Vincent) determined by Sr diffusion systematics. *Contrib. Mineral. Petrol.* **136**, 345–357 (1999).
70. de Maisonneuve, C. B. et al. How do olivines record magmatic events? Insights from major and trace element zoning. *Contrib. Mineral. Petrol.* **171**, 56 (2016).
71. Shea, T., Lynn, K. J. & Garcia, M. O. Cracking the olivine zoning code: distinguishing between crystal growth and diffusion. *Geology* **43**, 935–938 (2015).
72. Petrone, C. M., Bugatti, G., Braschi, E. & Tommasini, S. Pre-eruptive magmatic processes re-timed using a non-isothermal approach to magma chamber dynamics. *Nat. Commun.* **7**, 12946 (2016).
73. Cooper, K. M. & Kent, A. J. R. Rapid remobilization of magmatic crystals kept in cold storage. *Nature* **506**, 480–483 (2014).
Introduced the idea of 'cold storage' of magma, where crystals spend most of their lifetimes close to or under the magma solidus, as a way to explain the differences between the zircon ages and the timescales obtained from geospeedometry.
74. Mutch, E. J. F., Maclennan, J., Holland, T. J. B. & Buisman, I. Millennial storage of near-Moho magma. *Science* **365**, 260–264 (2019).
75. Putirka, K. D. Thermometers and barometers for volcanic systems. *Rev. Mineral. Geochem.* **69**, 61–120 (2008).
76. Kahl, M., Chakraborty, S., Costa, F. & Pompilio, M. Dynamic plumbing system beneath volcanoes revealed by kinetic modeling, and the connection to monitoring data: an example from Mt. Etna. *Earth Planet. Sci. Lett.* **308**, 11–22 (2011).
Links diffusion timescales obtained from crystals with monitoring time-series data of volcanoes to better understand the structure and time evolution of the system leading up to eruption.
77. Lynn, K. J., Garcia, M. O., Shea, T., Costa, F. & Swanson, D. A. Timescales of mixing and storage for Keanakāko'i Tephra magmas (1500–1820 C.E.), Kīlauea Volcano, Hawai'i. *Contrib. Mineral. Petrol.* **172**, 76 (2017).
78. Rae, A. S. P. et al. Time scales of magma transport and mixing at Kīlauea Volcano, Hawai'i. *Geology* **44**, 463–466 (2016).
79. Ruth, D. C. S. et al. Crystal and melt inclusion timescales reveal the evolution of magma migration before eruption. *Nat. Commun.* **9**, 2657–2657 (2018).
80. Chakraborty, S. Diffusion coefficients in olivine, wadsleyite and ringwoodite. *Rev. Mineral. Geochem.* **72**, 603–639 (2010).
81. Siebert L. & Simkin T. in *Global Volcanism Program Digital Information Series, GVP-3* (Smithsonian Institution, 2013)
82. Pankhurst, M. J., Morgan, D. J., Thordarson, T. & Loughlin, S. C. Magmatic crystal records in time, space, and process, causatively linked with volcanic unrest. *Earth Planet. Sci. Lett.* **493**, 231–241 (2018).
83. Kahl, M. et al. Compositionally zoned crystals and real-time degassing data reveal changes in magma transfer dynamics during the 2006 summit eruptive episodes of Mt. Etna. *Bull. Volcanol.* **75**, 692 (2013).
84. Rasmussen, D. J. et al. When does eruption run-up begin? Multidisciplinary insight from the 1999 eruption of Shishaldin volcano. *Earth Planet. Sci. Lett.* **486**, 1–14 (2018).
85. Albert, H., Costa, F. & Martí, J. Years to weeks of seismic unrest and magmatic intrusions precede monogenetic eruptions. *Geology* **44**, 211–214 (2016).
86. Ruprecht, P. & Plank, T. Feeding andesitic eruptions with a high-speed connection from the mantle. *Nature* **500**, 68–72 (2013).
87. Bebbington, M. S. Assessing spatio-temporal eruption forecasts in a monogenetic volcanic field. *J. Volcanol. Geotherm. Res.* **252**, 14–28 (2013).
88. Brenna, M. et al. Olivine xenocryst diffusion reveals rapid monogenetic basaltic magma ascent following complex storage at Pupuke Maar, Auckland Volcanic Field, New Zealand. *Earth Planet. Sci. Lett.* **499**, 13–22 (2018).
89. Demouchy, S., Jacobsen, S. D., Gaillard, F. & Stern, C. R. Rapid magma ascent recorded by water diffusion profiles in mantle olivine. *Geology* **34**, 429–432 (2006).
90. Barth, A. et al. Magma decompression rate correlates with explosivity at basaltic volcanoes — constraints from water diffusion in olivine. *J. Volcanol. Geotherm. Res.* **387**, 106664 (2019).
91. Ferguson, D. J. et al. Magma decompression rates during explosive eruptions of Kīlauea volcano, Hawaii, recorded by melt embayments. *Bull. Volcanol.* **78**, 71 (2016).
92. Oppenheimer, C. *Eruptions That Shook the World* (Cambridge Univ. Press, 2011).
93. Bachmann, O. & Huber, C. Silicic magma reservoirs in the Earth's crust. *Am. Mineral.* **101**, 2377–2404 (2016).
94. Rubin, A. E. et al. Rapid cooling and cold storage in a silicic magma reservoir recorded in individual crystals. *Science* **356**, 1154–1156 (2017).
Reports timescales from diffusion chronometry and dating of zircon from the same crystal zones. The results of long storage at low temperature generated significant discussion, especially for the application of Li diffusion in zircon.
95. Druitt, T. H., Costa, F., Deloule, E., Dungan, M. & Scaillet, B. Decadal to monthly timescales of magma transfer and reservoir growth at a caldera volcano. *Nature* **482**, 77–80 (2012).
96. Chamberlain, K. J., Morgan, D. J. & Wilson, C. J. N. Timescales of mixing and mobilisation in the Bishop Tuff magma body: perspectives from diffusion chronometry. *Contrib. Mineral. Petrol.* **168**, 1034 (2014).
97. Myers, M. L., Wallace, P. J., Wilson, C. J. N., Morter, B. K. & Swallow, E. J. Prolonged ascent and episodic venting of discrete magma batches at the onset of the Huckleberry Ridge supereruption, Yellowstone. *Earth Planet. Sci. Lett.* **451**, 285–297 (2016).
98. Myers, M. L., Wallace, P. J., Wilson, C. J. N., Watkins, J. M. & Liu, Y. Ascent rates of rhyolitic magma at the onset of three caldera-forming eruptions. *Am. Mineral.* **103**, 952–965 (2018).
99. Reid, M. R., Coath, C. D., Mark Harrison, T. & McKeegan, K. D. Prolonged residence times for the youngest rhyolites associated with Long Valley Caldera: 230Th—238U ion microprobe dating of young zircons. *Earth Planet. Sci. Lett.* **150**, 27–39 (1997).
100. Simon, J. I. & Reid, M. R. The pace of rhyolite differentiation and storage in an 'archetypical' silicic magma system, Long Valley, California. *Earth Planet. Sci. Lett.* **235**, 123–140 (2005).
101. Costa, F. in *Caldera Volcanism: Analysis, Modelling and Response* Vol. 10 (eds Gottsmann, J. & Martí, J.) 1–55 (Elsevier, 2008).
102. Turner, S. & Costa, F. Measuring timescales of magmatic evolution. *Elements* **3**, 267–272 (2007).
103. Barboni, M. et al. Warm storage for arc magmas. *Proc. Natl Acad. Sci. USA* **113**, 13959–13964 (2016).
104. Kaiser, J. F., de Silva, S., Schmitt, A. K., Economos, R. & Sunagua, M. Million-year melt–presence in monotonous intermediate magma for a volcanic–plutonic assemblage in the Central Andes: contrasting histories of crystal-rich and crystal-poor super-sized silicic magmas. *Earth Planet. Sci. Lett.* **457**, 73–86 (2017).
105. Miller, C. F. Eruptible magma. *Proc. Natl Acad. Sci. USA* **113**, 13941–13943 (2016).
106. Bindeman, I. N. & Melnik, O. E. Zircon survival, rebirth and recycling during crustal melting, magma crystallization, and mixing based on numerical modelling. *J. Petrol.* **57**, 437–460 (2016).
107. Feigl, K. L. et al. Rapid uplift in Laguna del Maule volcanic field of the Andean southern volcanic zone (Chile) 2007–2012. *Geophys. J. Int.* **196**, 885–901 (2014).
108. Sparks, R. S. J. et al. Uturuncu volcano, Bolivia: volcanic unrest due to mid-crustal magma intrusion. *Am. J. Sci.* **308**, 727–769 (2008).
109. Crank, J. *The Mathematics of Diffusion* 2nd edn (Oxford Univ. Press, 1975).
110. Girona, T. & Costa, F. DIPRA: a user-friendly program to model multi-element diffusion in olivine with applications to timescales of magmatic processes. *Geochem. Geophys. Geosyst.* **14**, 422–431 (2013).

111. Demouchy, S. & Mackwell, S. Mechanisms of hydrogen incorporation and diffusion in iron-bearing olivine. *Phys. Chem. Miner.* **33**, 347–355 (2006).
112. Jollands, M. C., Burnham, A., O'Neill, H. S. C., Hermann, J. & Qian, Q. Beryllium diffusion in olivine: a new tool to investigate timescales of magmatic processes. *Earth Planet. Sci. Lett.* **450**, 71–82 (2016).
113. Holzapfel, C., Chakraborty, S., Rubie, D. C. & Frost, D. J. Effect of pressure on Fe–Mg, Ni and Mn diffusion in $(Fe_xMg_{1-x})_2SiO_4$ olivine. *Phys. Earth Planet. Inter.* **162**, 186–198 (2007).
114. Jollands, M. C. et al. Substitution and diffusion of Cr^{2+} and Cr^{3+} in synthetic forsterite and natural olivine at 1200–1500 °C and 1 bar. *Geochim. Cosmochim. Acta* **220**, 407–428 (2018).
115. Coogan, L. A., Hain, A., Stahl, S. & Chakraborty, S. Experimental determination of the diffusion coefficient for calcium in olivine between 900 °C and 1500 °C. *Geochim. Cosmochim. Acta* **69**, 3683–3694 (2005).
116. Watson, E. B., Cherniak, D. J. & Holycross, M. E. Diffusion of phosphorus in olivine and molten basalt. *Am. Mineral.* **100**, 2053–2065 (2015).
117. Van Orman, J. A., Cherniak, D. J. & Kita, N. T. Magnesium diffusion in plagioclase: dependence on composition, and implications for thermal resetting of the ^{26}Al–^{26}Mg early solar system chronometer. *Earth Planet. Sci. Lett.* **385**, 79–88 (2014).
118. Giletti, B. J. & Casserly, J. E. D. Strontium diffusion kinetics in plagioclase feldspars. *Geochim. Cosmochim. Acta* **58**, 3785–3793 (1994).
119. Cherniak, D. J. Ba diffusion in feldspar. *Geochim. Cosmochim. Acta* **66**, 1641–1650 (2002).
120. Grove, T. L., Baker, M. B. & Kinzler, R. J. Coupled CaAl-NaSi diffusion in plagioclase feldspar: experiments and applications to cooling rate speedometry. *Geochim. Cosmochim. Acta* **48**, 2113–2121 (1984).
121. Dohmen, R., Ter Heege, J. H., Becker, H. W. & Chakraborty, S. Fe-Mg interdiffusion in orthopyroxene. *Am. Mineral.* **101**, 2210–2221 (2016).
122. Ferriss, E., Plank, T. & Walker, D. Site-specific hydrogen diffusion rates during clinopyroxene dehydration. *Contrib. Mineral. Petrol.* **171**, 55 (2016).
123. Müller, T., Dohmen, R., Becker, H. W., ter Heege, J. H. & Chakraborty, S. Fe–Mg interdiffusion rates in clinopyroxene: experimental data and implications for Fe–Mg exchange geothermometers. *Contrib. Mineral. Petrol.* **166**, 1563–1576 (2013).
124. Cherniak, D. J., Watson, E. B. & Wark, D. A. Ti diffusion in quartz. *Chem. Geol.* **236**, 65–74 (2007).
125. Tailby, N. D., Cherniak, D. J. & Watson, E. B. Al diffusion in quartz. *Am. Mineral.* **103**, 839–847 (2018).
126. Hartley, M. E., Morgan, D. J., Maclennan, J., Edmonds, M. & Thordarson, T. Tracking timescales of short-term precursors to large basaltic fissure eruptions through Fe–Mg diffusion in olivine. *Earth Planet. Sci. Lett.* **439**, 58–70 (2016).
127. Singer, B. S., Costa, F., Herrin, J. S., Hildreth, W. & Fierstein, J. The timing of compositionally-zoned magma reservoirs and mafic 'priming' weeks before the 1912 Novarupta-Katmai rhyolite eruption. *Earth Planet. Sci. Lett.* **451**, 125–137 (2016).
128. Longpré, M.-A., Klügel, A., Diehl, A. & Stix, J. Mixing in mantle magma reservoirs prior to and during the 2011–2012 eruption at El Hierro, Canary Islands. *Geology* **42**, 315–318 (2014).
129. Kahl, M., Chakraborty, S., Pompilio, M. & Costa, F. Constraints on the nature and evolution of the magma plumbing system of Mt. Etna volcano (1991–2008) from a combined thermodynamic and kinetic modelling of the compositional record of minerals. *J. Petrol.* **56**, 2025–2068 (2015).
130. Kahl, M., Viccaro, M., Ubide, T., Morgan, D. J. & Dingwell, D. B. A branched magma feeder system during the 1669 eruption of Mt Etna: evidence from a time-integrated study of zoned olivine phenocryst populations. *J. Petrol.* **58**, 443–472 (2017).
131. Albert, H. et al. Magma interactions, crystal mush formation, timescales, and unrest during caldera collapse and lateral eruption at ocean island basaltic volcanoes (Piton de la Fournaise, La Réunion). *Earth Planet. Sci. Lett.* **515**, 187–199 (2019).
132. Gordeychik, B. et al. Growth of, and diffusion in, olivine in ultra-fast ascending basalt magmas from Shiveluch volcano. *Sci. Rep.* **8**, 11775 (2018).
133. Morgado, E. et al. Transient shallow reservoirs beneath small eruptive centres: constraints from Mg-Fe interdiffusion in olivine. *J. Volcanol. Geotherm. Res.* **347**, 327–336 (2017).
134. Moussallam, Y. et al. Fast ascent rate during the 2017–2018 Plinian eruption of Ambae (Aoba) volcano: a petrological investigation. *Contrib. Mineral. Petrol.* **174**, 90 (2019).
135. Oeser, M., Ruprecht, P. & Weyer, S. Combined Fe-Mg chemical and isotopic zoning in olivine constraining magma mixing-to-eruption timescales for the continental arc volcano Irazú (Costa Rica) and Cr diffusion in olivine. *Am. Mineral.* **103**, 582–599 (2018).
136. Costa, F., Andreastuti, S., Bouvet de Maisonneuve, C. & Pallister, J. S. Petrological insights into the storage conditions, and magmatic processes that yielded the centennial 2010 Merapi explosive eruption. *J. Volcanol. Geotherm. Res.* **261**, 209–235 (2013).
137. Pan, Y. & Batiza, R. Mid-ocean ridge magma chamber processes: constraints from olivine zonation in lavas from the East Pacific Rise at 9°30′N and 10°30′N. *J. Geophys. Res. Solid Earth* **107**, ECV9–ECV9-13 (2002).
138. Zellmer, G. F. et al. Crystal growth during dike injection of MOR basaltic melts: evidence from preservation of local Sr disequilibria in plagioclase. *Contrib. Mineral. Petrol.* **161**, 153–173 (2011).
139. Moore, A., Coogan, L. A., Costa, F. & Perfit, M. R. Primitive melt replenishment and crystal-mush disaggregation in the weeks preceding the 2005–2006 eruption 9°50′N, EPR. *Earth Planet. Sci. Lett.* **403**, 15–26 (2014).
140. Andersen, N. L. et al. Petrochronologic perspective on rhyolite volcano unrest at Laguna del Maule, Chile. *Earth Planet. Sci. Lett.* **493**, 57–70 (2018).
141. Saunders, K., Blundy, J., Dohmen, R. & Cashman, K. Linking petrology and seismology at an active volcano. *Science* **336**, 1023–1027 (2012).
142. Morgan, D. J. et al. Time scales of crystal residence and magma chamber volume from modelling of diffusion profiles in phenocrysts: Vesuvius 1944. *Earth Planet. Sci. Lett.* **222**, 933–946 (2004).
143. Morgan, D. J. et al. Magma chamber recharge at Vesuvius in the century prior to the eruption of A.D. 79. *Geology* **34**, 845–848 (2006).
144. Costa, F. & Chakraborty, S. Decadal time gaps between mafic intrusion and silicic eruption obtained from chemical zoning patterns in olivine. *Earth Planet. Sci. Lett.* **227**, 517–530 (2004).
145. Allan, Aidan. S. R. et al. A cascade of magmatic events during the assembly and eruption of a super-sized magma body. *Contrib. Mineral. Petrol.* **172**, 49 (2017).
146. Barker, S. J., Wilson, C. J. N., Morgan, D. J. & Rowland, J. V. Rapid priming, accumulation, and recharge of magma driving recent eruptions at a hyperactive caldera volcano. *Geology* **44**, 323–326 (2016).
147. Matthews, N. E., Huber, C., Pyle, D. M. & Smith, V. C. Timescales of magma recharge and reactivation of large silicic systems from Ti diffusion in quartz. *J. Petrol.* **53**, 1385–1416 (2012).
148. Fabbro, G. N., Druitt, T. H. & Costa, F. Storage and eruption of Silicic magma across the transition from dominantly effusive to caldera-forming states at an arc volcano (Santorini, Greece). *J. Petrol.* **58**, 2429–2464 (2018).
149. Flaherty, T. et al. Multiple timescale constraints for high-flux magma chamber assembly prior to the Late Bronze Age eruption of Santorini (Greece). *Contrib. Mineral. Petrol.* **173**, 75 (2018).
150. Frontiers. Crystal Archives of Magmatic Processes. *frontiersin.org* https://www.frontiersin.org/research-topics/10167/crystal-archives-of-magmatic-processes#overview (2020).

Acknowledgements
F.C. acknowledges a Singapore National Research Foundation Investigatorship award (grant number NRF-NRFI2017-06). T.U. acknowledges funding from The University of Queensland (UQ-FREA RM2019001828 and UQ-MRFF RM2016000555). T.S. is supported by the National Science Foundation (NSF EAR grant 1725321).

Author contributions
F.C. wrote the manuscript, with contributions from T.S. and T.U. T.S. drafted the figures, with contributions from T.U. and F.C.

Competing interests
The authors declare no competing interests.

Peer review information
Nature Reviews Earth & Environment thanks J. Maclennan, K. Cooper, E. Bravo and M. Newcombe for their contribution to the peer review of this work.

Publisher's note
Springer Nature remains neutral with regard to jurisdictional claims in published maps and institutional affiliations.